Nat. Hazards Earth Syst. Sci. Discuss., 2, 4685–4710, 2014
www.nat-hazards-earth-syst-sci-discuss.net/2/4685/2014/
doi:10.5194/nhessd-2-4685-2014

Natural Hazards and Earth System Sciences
Open Access
Discussions

Relating weak layer and slab properties to snow slope stability

J. Schweizer and B. Reuter

WSL Institute for Snow and Avalanche Research SLF, Flüelastrasse 11,
7250 Davos Dorf, Switzerland

Received: 2 July 2014 – Accepted: 13 July 2014 – Published: 22 July 2014

Correspondence to: J. Schweizer (schweizer@slf.ch)

Published by Copernicus Publications on behalf of the European Geosciences Union.

Abstract

Snow slope stability evaluation requires considering weak layer as well as slab properties – and in particular their interaction. We developed a stability index from snow micro-penetrometer measurements and compared it to 129 concurrent point observations with the compression test (CT). The index considers the SMP-derived micro-structural strength and the additional load which depends on the hardness of the surface layers. The new quantitative measure of stability discriminated well between point observations rated as either "poor" or "fair" (CT < 19) and those rated as "good" (CT ≥ 19). However, discrimination power within the intermediate range was low. We then applied the index to gridded snow micro-penetrometer measurements from 11 snow slopes to explore the spatial structure and possibly relate it to slope stability. Stability distributions on the 11 slopes reflected various possible strength and load (stress) distributions that naturally can occur. Their relation to slope stability was poor possibly because the index does not consider crack propagation. Hence, the relation between spatial patterns of point stability and slope stability remains elusive. Whereas this is the first attempt of a truly quantitative measure of stability, future developments should consider a better reference of stability and incorporate a measure of crack propagation.

1 Introduction

Snow stability data are among the key ingredients when establishing avalanche forecasts. Snow stability can either be assessed from observations of instability such as recent avalanching (Jamieson et al., 2009), by stability tests performed in the field (e.g. Schweizer and Jamieson, 2010) or from stability indices derived from modelled snow stratigraphy (e.g. Durand et al., 1999; Schweizer et al., 2006). Whereas numerical modelling allows obtaining data with a high temporal and spatial resolution – though often of unknown accuracy, field tests are laborious and reveal partly subjective point information of low temporal and spatial resolution. Nevertheless, stability tests are presently

NHESSD
2, 4685–4710, 2014

the method of choice for estimating snow stability – despite the fact that the inherently variable nature of the mountain snowpack hinders extrapolation of point observations (Schweizer et al., 2008). One way to overcome the limitation of point observations is to perform many measurements in a given area within a couple of hours. This approach is only possible with a quick probing method, for example, with the snow micro-penetrometer (Schneebeli and Johnson, 1998) or potentially with remote sensing techniques.

The snow micro-penetrometer (SMP) is a probe with a high-resolution force sensor at its tip driven into the snowpack at constant speed. It provides a penetration resistance (force)-depth signal that includes micro-structural information (Johnson and Schneebeli, 1999; Marshall and Johnson, 2009). Mechanical properties can be derived from the three basic micro-structural parameters: element length (L), deflection at rupture (δ), and rupture force (f). The micro-structural strength (σ_m) is assumed to scale as f/L^2.

In one of the first attempts to relate the SMP resistance to stability Kronholm (2004) found increasing stability scores with increasing weak layer penetration resistance for four out of five investigated weak layers. Based on the characteristics found in manually observed snow profiles (Schweizer and Jamieson, 2007), Pielmeier and Schweizer (2007) tried to discriminate between unstable and stable observations based on SMP derived characteristics of the weak layer and the adjacent layers. Pielmeier and Marshall (2009) refined this approach and showed that the micro-structural strength of the weak layer (manually identified in the SMP profile) was the single best classifier to discriminate between unstable and stable Rutschblock test results. Classification accuracy improved to about 85 % when SMP-derived mean slab density (Pielmeier, 2003) was included in a 2-node classification tree. They pointed out the importance of signal quality control and showed the improvement in classification accuracy that can be obtained when several SMP measurements within an area of a few m^2 are performed. Lutz et al. (2009) and Bellaire and Schweizer (2011) also found the micro-structural strength of the weak layer to be related to stability. Floyer

NHESSD
2, 4685–4710, 2014

and Jamieson (2009) predicted the fracture character of compression tests from adjacent SABRE penetrometer profiles, whereas van Herwijnen et al. (2009) found snow stratigraphy derived from micro-structural properties of the SMP to be related to the fracture type in compression tests.

Direct correlations of point measurements such as SMP penetration hardness to stability have proven challenging (Lutz et al., 2009). Previous studies of many point measurements at the slope scale using the SMP revealed, among other things, that typical weak layers are often continuously present, but have clearly varying properties (e.g. Kronholm et al., 2004). However, relating spatial variations as derived from point measurements to slope stability has so far not been successful. For example, Bellaire and Schweizer (2011) stated that firm conclusions on the dependence of slope stability on spatial variations were not possible due to the limited range of snow conditions in the dataset, and the fact that the definition of slope stability is partly intangible. From a theoretical point of view, as supported by numerical modelling (e.g. Fyffe and Zaiser, 2004; Gaume et al., 2013; Kronholm and Birkeland, 2005), it seems clear that stability variations at the slope scale can either promote or hinder slope failure. Slope instability should increase with increasing coefficient of variation and increasing correlation length.

Whereas the above mentioned studies indicate that considerable progress has been made towards objectively deriving snow stability information from the SMP resistance profile, a single measure of stability, combining slab and weak layer properties, is so far lacking. Also, relating point measurements to slope stability has not been successful. We will present a first attempt to directly derive an index of snow stability from the SMP signal and compare it to results of numerous small-scale stability tests (Compression Test). The index will then be applied to the gridded SMP measurements collected on 11 slopes by Bellaire and Schweizer (2011) to explore the spatial structure of stability on these slopes, and possibly relate it to slope stability. The index will at best be an estimate of the probability of initiating a failure in a weak layer, but will not provide any information on the propensity of crack propagation.

NHESSD
2, 4685–4710, 2014

2 Data

We primarily used the data collected and described by Bellaire and Schweizer (2011). They concurrently observed snow stability using the Compression Test (CT) (Jamieson, 1999) and measured penetration resistance using the SMP on 15 slopes above Davos, Switzerland during the winters 2006–2007 to 2007–2008. During the winter 2008–2009 Bellaire (2010) sampled another 8 slopes. On each of the slopes, one manually observed snow profile, 9 pairs of CT and 45 SMP measurements were performed. In addition, other observations relevant for assessing slope stability such as signs of instability, snow surface conditions and ski penetration were recorded. For the analysis described below, we used three different datasets out of these data from 23 slopes.

a. From the concurrent observations of point stability (CT) and penetration resistance (SMP), we analysed, after quality control, in total 129 SMP profiles with corresponding CT score.

b. From the 23 concurrent observations of snow stratigraphy (snow profile) and penetration resistance (SMP), 19 cases were retained after quality control.

c. From the gridded SMP data on 23 slopes, we analysed 11 slopes in regard to their stability distribution. Most of the remaining data could not be used for quality issues.

3 Methods

Our assumptions are tied to the compression test as we aim at a stability criterion for failure initiation which can be validated with previously collected field data. The stability index follows a simple strength to additional stress criterion in the weak layer still accounting for slab layering. In the compression test experiment a snow column is loaded by dropping the hand, the forearm or the arm (Jamieson, 1999). For simplicity

NHESSD
2, 4685–4710, 2014

we consider a fixed weight corresponding to the weight of a forearm. Due to the impact the surface layers are compacted or rather crushed (van Herwijnen and Birkeland, 2014). The stress in the column is related to the braking (or decelerating) distance. The softer the surface layers the larger is the compaction (and also the braking distance) and hence the smaller is the stress – and vice versa. We assumed idealized elastic-plastic behavior of the snow so that the initial potential energy E_{pot} of the dropping weight was completely dissipated over the braking distance:

$$E_{pot} = E_a = F_u u_{max} - F_u^2/2K \tag{1}$$

with E_a the dissipated energy which is equal to the area under the curve in the loading (force-displacement) diagram, F_u the maximum impact force, u_{max} the maximum displacement (i.e. the braking distance), and K the elastic modulus (Fig. 1). As the elastic part of deformation is negligibly small compared to the plastic deformation, the second term in Eq. (1) can be neglected. With $E_{pot} = mg\Delta h$ the impact force can then be approximated:

$$F_u \approx mg\Delta h/u_{max}. \tag{2}$$

Dividing the impact force by the area of the column A (0.3 m × 0.3 m) reveals the additional stress: $\Delta\sigma_g = F_u/A$. For the potential energy $mg\Delta h$, we assumed a weight of 1.5 kg dropping from a height of 0.15 m resulting in an energy of about 2.2 J; roughly corresponding to the impact by a falling forearm.

We assumed the braking distance u_{max} to be related to the penetration depth as measured with a penetrometer. In order to derive the penetration depth from the SMP signal we cumulated the SMP penetration force over depth to an a priori unknown threshold of dissipated energy (e_a). This implies that the area under the penetration force-depth curve corresponds to the dissipated energy e_a. Using the small dataset mentioned above ($N = 19$) with observed penetration depth (PS), we determined the dissipated energy up to the depth PS for each SMP profile:

NHESSD
2, 4685–4710, 2014

$$e_a = \int_0^{PS} F \, dh \tag{3}$$

with F the penetration force and h the depth from the snow surface. The average energy e_a absorbed up to the penetration depth PS was 0.036 N m. In the following, we used this threshold value to calculate the SMP derived penetration depth (or breaking distance) (ps). For the 19 cases the median deviation between observed (PS) and modeled (ps) penetration depth was 1.5 cm, with one outlier of 8.4 cm (standard error: 2.5 cm) (Fig. 2).

For calculating the stability index, we assumed that the additional stress (derived from Eq. 2) would not decrease strongly with depth as the snow column is uniformly loaded at the top. Furthermore, we neglected the weight of the overlying slab (which is e.g. considered in the skier stability index introduced by Föhn (1987) as we suppose that the dynamic load (rather than the static load) is essential for initiating a failure due to the well-known deformation rate dependence of snow strength (e.g. Narita, 1980). Finally, we did not consider the effect of slope angle on either stress or strength as its effect is largely unknown in the case of a compression test.

The simple stability index was defined as:

$$S = \frac{\sigma_m}{\Delta\sigma}. \tag{4}$$

Hence we assume that SMP derived stability S is simply proportional to the micro-structural strength σ_m and the SMP derived penetration depth ps: $S \sim \sigma_m$ ps. The above definition of the stability index (Eq. 4) yields values that are not comparable to the classical stability index where a value less than 1 (to 1.5) indicates instability (Jamieson and Johnston, 1998) – but the proposed stability index could easily be normalized.

We related the newly developed stability index to the compression test scores and assessed the correlation with the Spearman rank order coefficient. As suggested by

NHESSD
2, 4685–4710, 2014

Bellaire and Schweizer (2011) CT scores were classified into three point stability classes "poor", "fair" and "good" (Table 1). Similarly, all slopes were classified into one of three classes of slope stability "POOR", "FAIR" and "GOOD". The classification considered the presence or absence of signs of instability and the slope median CT score; in contrast to Bellaire and Schweizer (2011) we did not consider the profile classification (Table 2). The stability distributions were characterized by the median, the interquartile range (IQR) and the quartile coefficient of variation (QCV). When comparing the distributions of stability index from the three point stability classes, the non-parametric Kruskall–Wallis H test was used. A level of significance $p = 0.05$ was chosen to decide whether the observed differences were statistically significant. Split values between two categories were determined with the classification tree method (Breiman et al., 1998). To assess the classification accuracy the probability of detection (POD), the probability of non-events (PON) and the true skill statistic TSS (i.e. the difference between POD and the false alarm rate) were calculated (Wilks, 2011). To explore the spatial structure the experimental semivariogram for a linear trend model of the Cartesian coordinates was calculated. By fitting a spherical model to the experimental semivariogram we determined the range which is a measure of the correlation length. Details are given in Bellaire and Schweizer (2011). For contour plots data were interpolated by ordinary kriging.

4 Results

The newly developed stability index was calculated for the dataset of the 129 cases with SMP profile and CT score (Fig. 3). The Spearman rank correlation coefficient between CT score and stability index S was $r_s = 0.42$ ($p < 0.001$) slightly higher than for the micro-structural strength ($r_s = 0.31$; $p < 0.001$). Correlating the median stability for each CT score yielded $r_s = 0.77$ ($p < 0.001$).

Grouping the stability values according to the three classes of point stability indicated that in particular the tests rated as "poor" can well be discriminated from those

NHESSD
2, 4685–4710, 2014

rated as "good" (Fig. 4). In fact, differences between all three classes, also between "poor" and "fair", were judged to be statistically significant ($p < 0.001$, pairwise U test). If the classes of "poor" and "fair" are grouped the classification simplifies and becomes comparable to previous studies (e.g. Pielmeier and Marshall, 2009). With a split value of 212, the classification accuracy (10-fold cross-validated) was 81 % ($N = 129$; POD: 78 %, PON: 89 %, TSS: 68 %).

4.1 Non-spatial analysis

The stability distributions found on the 11 slopes were fairly different (Fig. 5); only those stability values are shown in Fig. 5 where concurrently an SMP measurement and a compression test was performed. The four slopes that were rated "POOR" had low stability and a low mean CT score. The two slopes rated as "FAIR" had similarly low stability and mean CT scores, but were not rated as "POOR" since no signs of instability were observed. Three of the slopes rated as "GOOD" had still relatively low stability and intermediate CT scores, whereas the other two slopes had high stability as well as high CT scores. Overall, per slope, the median stability was still positively, but not significantly correlated with the median CT score ($r_s = 0.47$, $p = 0.15$).

The different stability distributions were the result of various, different stress-strength (slab-weak layer) configurations (Fig. 6). For example, grid 0708_9 had rather low strength (53 kPa), but due to the low additional stress (151 Pa), the stability was relatively high (355). On the other hand, grid 0607_6 had rather low stability (167), though the weak layer strength was intermediate (95 kPa), but the additional stress was high (561 Pa).

Considering all SMP measurements in the 11 grids (Table 3), the median stability index tended to increase with increasing median CT score, but the correlation was not significant ($r_s = 0.36$, $p = 0.28$). The stability index was only slightly higher for the slopes rated as "GOOD" (median stability: 145) compared to the slopes rated as either "POOR" or "FAIR" (median stability: 123). Most grids had a median stability index in the range of about 100 to 170, and the slope stability rating was mostly "POOR" or "FAIR"

NHESSD
2, 4685–4710, 2014

with 3 cases of "GOOD". In the latter three cases no signs of instability were observed – explaining the discrepancy. The two grids with high median stability were rated as "GOOD". One of these grids (0708_7) that showed a rather low median stability index (104), but was rated as "GOOD", had the largest variations in stability (QCV = 0.43). The large variations resulted from large variations in slab properties. As shown in Fig. 6, the stability index depended on the slab and the weak layer properties. For example, the four grids 0708_1, 0708_3, 0708_5 and 0708_9 had all fairly low strength, but stability in terms of median CT score largely differed; the first two were rather unstable whereas the latter two of those four grids were rather stable.

In most grids, stability values were either rated rather "stable" or "unstable". The two grids 0708_6 and 0708_9 had 0 and 4 % "unstable" stability values, in in the other cases more than 75 % of the stability values were below the stable-unstable threshold ($S \leq 212$). Mixed results, i.e. about half of the stability index values rather stable, the other half rather unstable were not observed.

The variation within a grid, expressed as the quartile coefficient of variation, was typically largest for stability (mean QCV = 0.28), and lowest for strength (mean QCV = 0.18). However, the differences were statistically not significant (H test, $p = 0.11$). The QCV and the range were not related to the median stability. The range tended to decrease with increasing QCV, but the trend was statistically not significant ($p = 0.43$).

The slope median stability index was positively related with the slope median strength of the weak layer ($r_c = 0.76$, $p = 0.02$) indicating that stability is in general largely influenced by strength, and much less so by the stress (load) ($r_c = -0.47$, $p = 0.15$).

4.2 Spatial analysis

In most grids the variogram indicated that the range was less than 5 m (Table 3). The values of the range for stress (load), strength and stability varied on a given day. They were not significantly correlated – though the range for stability tended to increase with increasing range for strength ($r_c = 0.58$; $p = 0.06$). Furthermore, the stability range

NHESSD
2, 4685–4710, 2014

tended to be larger for the slopes rated as "GOOD" than for the slopes rated as either "POOR" or "FAIR", but the difference was small and statistically not significant (H test: $p = 0.7$).

Figure 7 illustrates for two grids the variable spatial structure of strength, stress and resulting stability. For grid 0708_3, when stability was low, the stress values did not show any particular trend or clustering; only the values towards the lower left and right corners tended to be slightly higher. For the stress a slope scale trend with some higher values towards the left can be observed. Stability was some higher in the lower left corner than in the higher left one. This observation can be explained by the trend for higher stress in the upper left corner and higher strength in the lower left corner. For the second grid (0708_6) in Fig. 7, some slope scale trends were observed for strength (higher values towards the right), stress (higher values towards the left), and accordingly for stability (higher values towards the right).

5 Discussion

The presented stability approach has to been seen as a rough estimate. The proposed stability index will at best be an estimate of the probability of initiating a failure in a weak layer, but will not provide any information on the propensity of crack propagation.

As many SMP measurements with concurrent compression test results were available, we used the CT as stability reference. Obviously this test is far from perfect (e.g. Winkler and Schweizer, 2009), but at least it is known that the CT score increases with decreasing probability of skier triggering (Jamieson, 1999). Some of the problems include the geometry (scale of length to width), unknown boundary effects and the stepwise loading with only three loading steps. Many factors that probably play a role, how important is mostly unknown, were not considered in our simple model for determining the additional stress acting at the depth of the weak layer. We considered the loading at the top of the column, the size of load according to the second loading step (tapping from the elbow), and the considerable compression of the surface layers. On

NHESSD
2, 4685–4710, 2014

the other hand, we did not consider the stratigraphy (apart from the surface layers), boundary effects, possible stress waves in the column or load dissipation with depth. As the column is loaded over the whole area, we assumed no load dissipation which is obviously important in the case of a point or a line load. Some recent measurements by Thumlert and Jamieson (2014) may question this assumption. Nevertheless, the derived stability index was clearly related to the stability reference we had at hand. As the micro-structural compressive strength has been shown to be related to stability (Pielmeier and Marshall, 2009) and the stability index is slightly better related to the CT score, further suggests that our index is indicative. However, as has been previously shown by Jamieson (1999) the CT does not differentiate well within the intermediate range (CT scores 11 to 20) so that our stability index is afflicted with the same problem. Accordingly, the correlation between the slope median CT score and the slope median stability index was rather poor, mainly since the sample size was small ($N = 11$) and most grids had a median CT score in the intermediate range.

Certainly, a better stability reference should allow developing a more sophisticated index along the lines of the skier stability index (SK38) (Jamieson and Johnston, 1998). The comparison to the various slope classifications has clearly shown that the index lacks any information about crack propagation propensity. The slopes rated as "FAIR" had mostly low stability, but no signs of instability were observed. In the future, the initiation index should be combined with a measure of crack propagation propensity, for example, the critical crack length that can be derived from the SMP signal (Reuter et al., 2013).

Non-spatial variations of strength, stress and stability expressed as the QCV were similar as found in previous slope-scale studies (Schweizer et al., 2008). Whereas Bellaire and Schweizer (2011) separately related weak and slab layer properties to slope stability, we jointly considered both properties by introducing a simple measure of stability. However, we were still not able to resolve the influence of spatial patterns on slope stability. One of the reasons we did not find any relation between spatial characteristics of point stability measurements and the slope stability estimate may be

NHESSD
2, 4685–4710, 2014

the lack of slopes exhibiting strong variations in stability, i.e. about equal shares of high and low stability values. In such situations one would expect that the spatial patterns of point stability characterized by its correlation length would control slope stability. A further reason may be that the proposed stability index only considers failure initiation and does not include crack propagation.

6 Conclusions

We have revisited the data collected by Bellaire and Schweizer (2011) and developed for the first time a measurement-based stability index. It combines weak layer strength (SMP-derived micro-structural strength) with a rough measure of the additional stress at the depth of the weak layer depending on the properties of the surface layers (i.e. slab layers) (SMP-derived penetration depth). The index was positively correlated with the results of compression tests performed concurrently with the SMP measurements. It discriminated well between point stabilities rated as either "poor" or "fair" and those rated as "good" with a 10-fold cross validated classification accuracy of about 80 %. A rich variety of stress, strength and stability scenarios was found indicating that the index, despite its simplicity, seems to be able to mimic at least some of the complex interactions between slab and weak layer properties. The well-known challenging problem of correlating variations in point stability to slope stability could not be solved – despite the fact that now at least a measure of stability exists. However, the target variable – slope stability – is not even well defined either.

In a next step we will seek a dataset with reference stability better suited than the CT, possibly the Rutschblock, and will combine a more sophisticated stability index, rather an initiation index, with a propagation propensity index, possibly the critical length as known from the propagation saw test.

Acknowledgements. We thank Sascha Bellaire for providing the data and Christoph Mitterer for help with some of the analysis.

References

Bellaire, S.: Spatial variability of the snow cover and its effect on avalanche formation, Ph.D. thesis, Department of Geosciences, University of Hamburg, Hamburg, Germany, 196 pp., 2010.

Bellaire, S. and Schweizer, J.: Measuring spatial variations of weak layer and slab properties with regard to snow slope stability, Cold Reg. Sci. Technol., 65, 234–241, 2011.

Breiman, L., Friedman, J. H., Olshen, R. A., and Stone, C. J.: Classification and Regression Trees, CRC Press, Boca Raton, USA, 1998.

Durand, Y., Giraud, G., Brun, E., Mérindol, L., and Martin, E.: A computer-based system simulating snowpack structures as a tool for regional avalanche forecasting, J. Glaciol., 45, 469–484, 1999.

Floyer, J. and Jamieson, B.: Predicting the fracture character of weak layers from snowpack penetrometer signals, Cold Reg. Sci. Technol., 59, 185–192, 2009.

Föhn, P. M. B.: The stability index and various triggering mechanisms, in: Symposium at Davos 1986 – Avalanche Formation, Movement and Effects, IAHS Publ. 162, edited by: Salm, B. and Gubler, H., International Association of Hydrological Sciences, Wallingford, Oxfordshire, UK, 195–214, 1987.

Fyffe, B. and Zaiser, M.: The effects of snow variability on slab avalanche release, Cold Reg. Sci. Technol., 40, 229–242, 2004.

Gaume, J., Schweizer, J., van Herwijnen, A., Chambon, G., Eckert, N., and Naaim, M.: The effect of spatial variations of snowpack properties on snow slope stability: a mechanically-based statistical approach, in: Proceedings ISSW 2013, International Snow Science Workshop, 7–11 October 2013, Grenoble, France, 57–60, 2013.

Jamieson, B., Haegeli, P., and Schweizer, J.: Field observations for estimating the local avalanche danger in the Columbia Mountains of Canada, Cold Reg. Sci. Technol., 58, 84–91, 2009.

Jamieson, J. B.: The compression test – after 25 years, Avalanche Review, 18, 10–12, 1999.

Jamieson, J. B. and Johnston, C. D.: Refinements to the stability index for skier-triggered dry slab avalanches, Ann. Glaciol., 26, 296–302, 1998.

Johnson, J. B. and Schneebeli, M.: Characterizing the microstructural and micromechanical properties of snow, Cold Reg. Sci. Technol., 30, 91–100, 1999.

Kronholm, K.: Spatial variability of snow mechanical properties with regard to avalanche formation, Ph.D. thesis, Faculty of Natural Sciences and Mathematics, University of Zurich, Zurich, Switzerland, 192 pp., 2004.
Kronholm, K. and Birkeland, K. W.: Integrating spatial patterns into a snow avalanche cellular automata model, Geophys. Res. Lett., 32, L19504, doi:10.1029/2005GL024373, 2005.
Kronholm, K., Schneebeli, M., and Schweizer, J.: Spatial variability of micropenetration resistance in snow layers on a small slope, Ann. Glaciol., 38, 202–208, 2004.
Lutz, E., Birkeland, K., and Marshall, H.-P.: Quantifying changes in weak layer microstructure associated with artificial load changes, Cold Reg. Sci. Technol., 59, 202–209, 2009.
Marshall, H.-P. and Johnson, J. B.: Accurate inversion of high-resolution snow penetrometer signals for microstructural and micromechanical properties, J. Geophys. Res., 114, F04016, doi:10.1029/2009jf001269, 2009.
Narita, H.: Mechanical behaviour and structure of snow under uniaxial tensile stress, J. Glaciol., 26, 275–282, 1980.
Pielmeier, C.: Textural and mechanical variability of mountain snowpacks, Ph.D. thesis, University of Berne, Berne, Switzerland, 127 pp., 2003.
Pielmeier, C. and Marshall, H.-P.: Rutschblock-scale snowpack stability derived from multiple quality-controlled SnowMicroPen measurements, Cold Reg. Sci. Technol., 59, 178–184, 2009.
Pielmeier, C. and Schweizer, J.: Snowpack stability information derived from the SnowMicroPen, Cold Reg. Sci. Technol., 47, 102–107, 2007.
Reuter, B., Proksch, M., Loewe, H., van Herwijnen, A., and Schweizer, J.: On how to measure snow mechanical properties relevant to slab avalanche release, in: Proceedings ISSW 2013, International Snow Science Workshop, 7–11 October 2013, Grenoble, France, 7–11, 2013.
Schneebeli, M. and Johnson, J. B.: A constant-speed penetrometer for high-resolution snow stratigraphy, Ann. Glaciol., 26, 107–111, 1998.
Schweizer, J. and Jamieson, J. B.: A threshold sum approach to stability evaluation of manual snow profiles, Cold Reg. Sci. Technol., 47, 50–59, 2007.
Schweizer, J. and Jamieson, J. B.: Snowpack tests for assessing snow-slope instability, Ann. Glaciol., 51, 187–194, 2010.
Schweizer, J., Bellaire, S., Fierz, C., Lehning, M., and Pielmeier, C.: Evaluating and improving the stability predictions of the snow cover model SNOWPACK, Cold Reg. Sci. Technol., 46, 52–59, 2006.

NHESSD
2, 4685–4710, 2014

Schweizer, J., Kronholm, K., Jamieson, J. B., and Birkeland, K. W.: Review of spatial variability of snowpack properties and its importance for avalanche formation, Cold Reg. Sci. Technol., 51, 253–272, 2008.

Thumlert, S. and Jamieson, B.: Stress measurements in the snow cover below localized dynamic loads, Cold Reg. Sci. Technol., 106–107, 28–75, 2014.

van Herwijnen, A. and Birkeland, K. W.: Measurements of snow slab displacement in extended column tests and comparison with propagation saw tests, Cold Reg. Sci. Technol., 97, 97–103, 2014.

van Herwijnen, A., Bellaire, S., and Schweizer, J.: Comparison of micro-structural snowpack parameters derived from penetration resistance measurements with fracture character observations from compression tests, Cold Reg. Sci. Technol., 59, 193–201, 2009.

Wilks, D. S.: Statistical Methods in the Atmospheric Sciences, Academic Press, San Diego, CA, USA, 2011.

Winkler, K. and Schweizer, J.: Comparison of snow stability tests: extended column test, rutschblock test and compression test, Cold Reg. Sci. Technol., 59, 217–226, 2009.

Wright, C.: Introduction to structural impact. in: PDHonline Course S164, PDH Online, available at: http://www.pdhcenter.com/courses/s164/s164content.pdf, last access: 2 July 2014, Fairfax, VA, USA, 2012.

NHESSD

2, 4685–4710, 2014

Relating weak layer and slab properties

J. Schweizer and B. Reuter

Table 1. Point stability classification based on CT score and CT fracture type.

CT score	CT fracture character	
	SP, SC	RP, PC, B
≤ 13	poor	fair
14 . . . 18	fair	fair
≥ 19	good	good

NHESSD
2, 4685–4710, 2014

Table 2. Slope stability classification based on the slope median point stability and signs of instability (recent avalanching, whumpfs of shooting cracks).

Median CT score	Signs of instability 1: present	0: absent
≤ 13	POOR	FAIR
> 13	FAIR	GOOD

NHESSD
2, 4685–4710, 2014

Table 3. Summary statistics for the eleven grids. For signs of instability "1" indicates presence, "0" absence of whumpfs, shooting cracks or recent avalanches. Proportion weak describes the portion of point stability measurements with $S \leq 212$.

Grid ID	Date	Median CT score	Signs of instability	Slope stability	Stability index				Range (m)		Proportion weak
					Median	IQR	QCV	Load	Strength	Stability	
0708_1	10 Jan 08	10.5	1	POOR	142	89	0.28	2.3	1.6	1.8	0.78
0708_3	23 Jan 08	11	1	POOR	108	75	0.31	3.2	8.8	9.1	0.95
0708_2	17 Jan 08	11.5	1	POOR	124	30	0.12	1.7	5.3	1.8	0.96
0607_6	15 Mar 07	12	1	POOR	167	110	0.33	1.8	0.2	2.7	0.74
0607_5	8 Mar 07	12	0	FAIR	35	17	0.24	1.2	1.7	1.4	1.0
0708_5	7 Feb 08	12.5	0	FAIR	123	102	0.41	4.3	1.9	4.0	0.80
0607_3	16 Feb 07	13.5	0	GOOD	145	55	0.18	1.1	5.5	5.6	0.78
0708_7	19 Feb 08	14	0	GOOD	104	106	0.43	9.2	2.8	2.6	0.90
0708_4	31 Jan 08	14.5	0	GOOD	122	78	0.28	1.3	9.6	3.5	0.87
0708_9	18 Mar 08	19	0	GOOD	355	75	0.11	2.0	1.2	1.5	0.04
0708_6	15 Feb 08	22.5	0	GOOD	928	691	0.37	2.3	7.4	2.9	0.0

NHESSD
2, 4685–4710, 2014

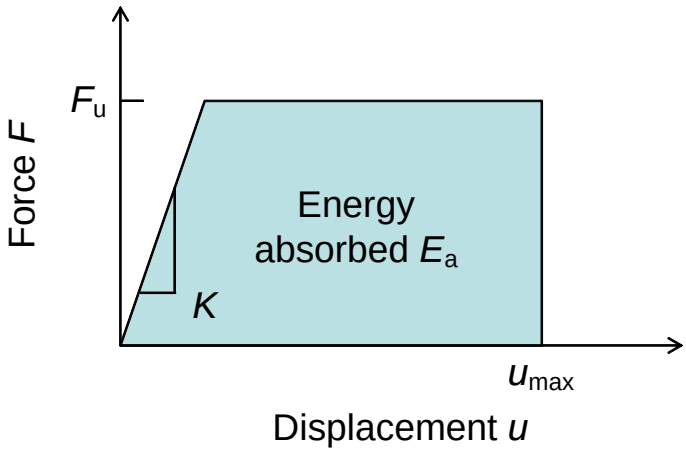

Figure 1. Schematic of elastic-plastic deformation describing the inelastic collision while loading the snow column in a Compression Test. K denotes the elastic (after Wright, 2012).

NHESSD
2, 4685–4710, 2014

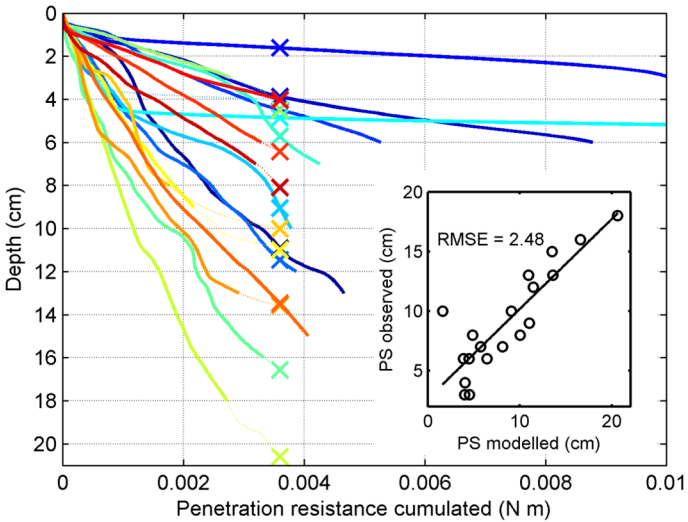

Figure 2. Cumulated penetration resistance (= dissipated energy) vs. depth for 19 SMP penetration resistance-depth signals. Solid lines show paths of cumulated penetration resistance up to observed penetration depth PS. Crosses denote corresponding depth (= modelled penetration depth ps) for average value of dissipated energy e_a = 0.0036 Nm. If observed PS is lower than modelled ps a dashed line leads from the end of the solid line to the corresponding cross. Inset shows modelled vs. observed penetration depth.

NHESSD
2, 4685–4710, 2014

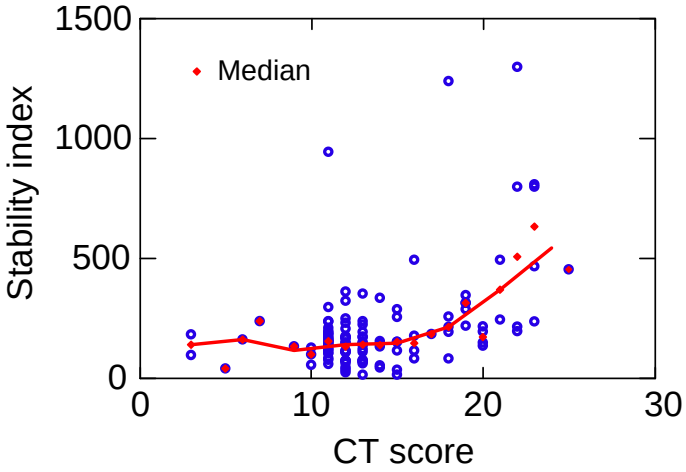

Figure 3. Stability index vs. CT score (8 cases with CT score 35 (= no fracture) not shown, N = 121); moving average smoothing line between median values.

NHESSD
2, 4685–4710, 2014

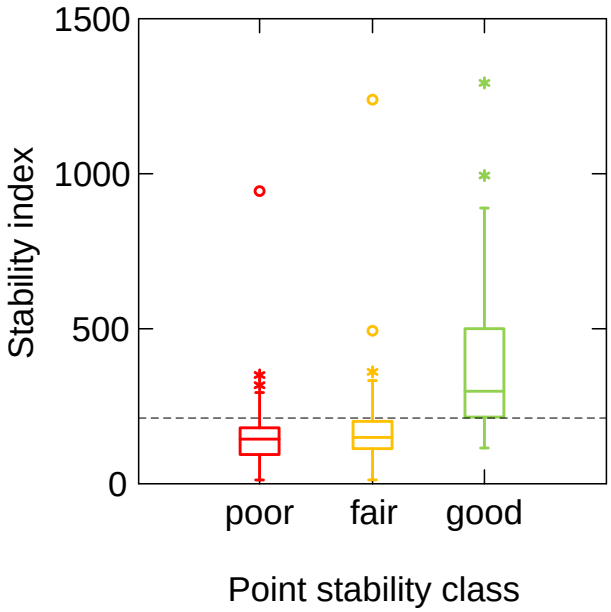

Figure 4. Stability index grouped into the three classes of point stability (based on CT score and fracture type) (N = 129; "poor": 70, "fair": 31, "good": 28). Dashed line indicates the split value for the classification into two classes ("poor" and "fair" vs. "good").

NHESSD
2, 4685–4710, 2014

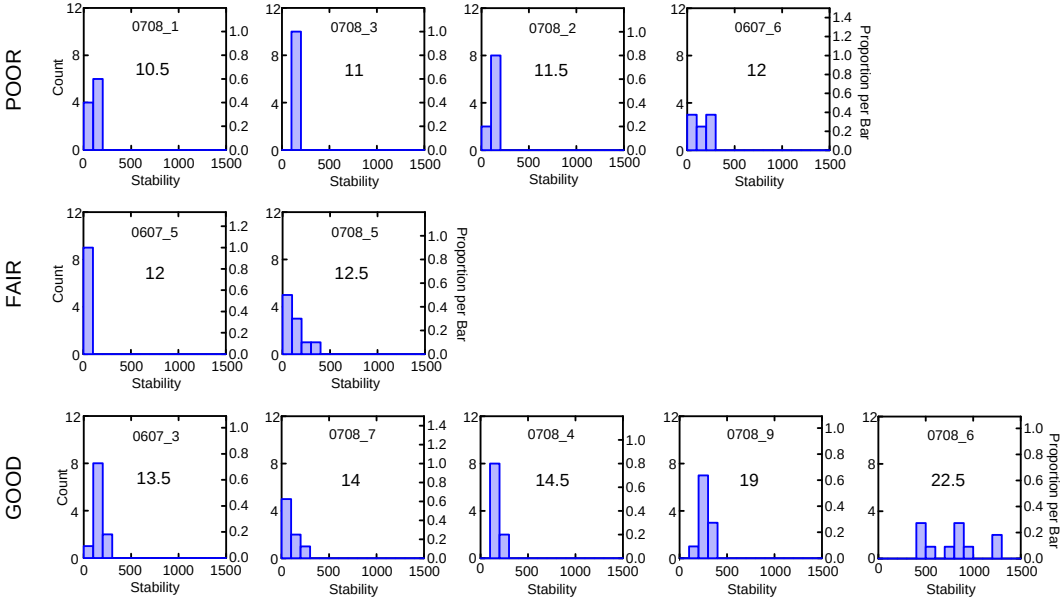

Figure 5. Stability distributions of the 11 slopes sampled during winters 2006–2007 and 2007–2008. Only stability derived from those SMP measurements with concurrent CT test are shown. Median CT score is indicated in the middle of each histogram. Slopes are ordered with regard to slope stability ("POOR", "FAIR", "GOOD") and within rows based on median CT score. *N* varies between 8 and 11.

NHESSD
2, 4685–4710, 2014

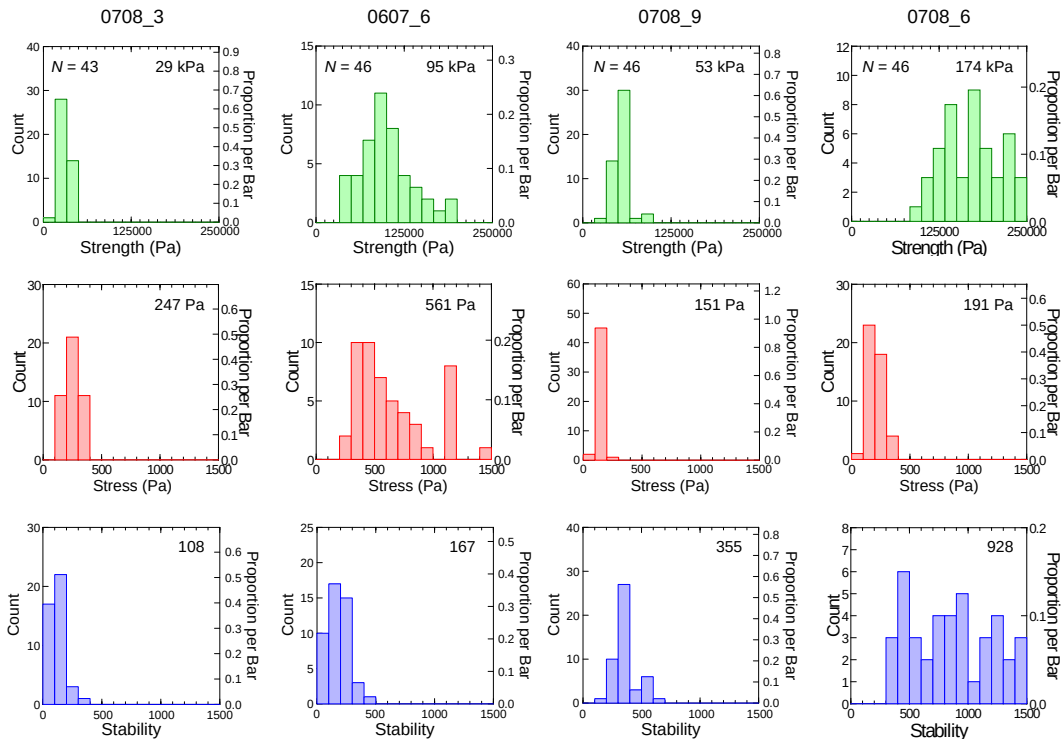

Figure 6. Exemplary strength, stress and stability distributions for four slopes (grids). Numbers indicate the median value. *N* varies between 43 and 46.

NHESSD
2, 4685–4710, 2014

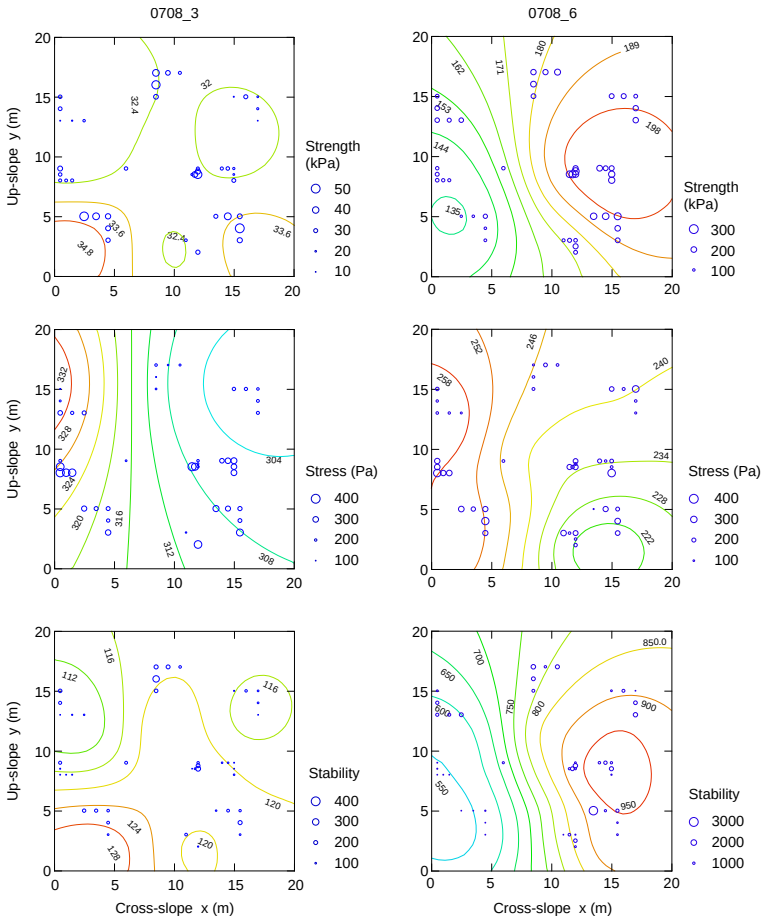

Figure 7. Contour plots of strength, stress (load) and stability for two grids in winter 2007–2008 (left: 0708_3, right: 0708_6).

NHESSD
2, 4685–4710, 2014